Observation of ice particle shape and orientation from ground-based remote sensing measurements, ICYHALO

Linda Forster

Introduction and motivation

Passive remote sensing provides invaluable information about ice cloud optical and microphysical properties. Missing knowledge about ice particle habit, however, introduces an uncertainty of at least a factor 2 in optical thickness retrievals. Any information about particle habit would therefore be extremely valuable for improving ice cloud remote sensing and for better quantifying the effect of ice clouds on the radiation budget and thus on climate. Ice particle shape and orientation produce distinct signals in the sky radiance distribution, which can be observed in a variety of halo displays. 22°-halos are a clear indication of randomly oriented hexagonal prisms while sundogs are produced by oriented hexagonal plates. The brightness contrast of the 22°-halo may therefore be used to retrieve quantitative information about the fraction of hexagonal ice crystals. Whereas the brightness of the sundog in comparison to the halo should further allow to determine the fraction of oriented particles.

Scientific objectives

To obtain a continuous time series of observations of different halo displays a sun-tracking wide-angle camera system (HaloCam) was installed at CESAR in Cabauw. The HaloCam observations provide continuous information about the temporal variability of halo displays and the derived fraction of hexagonal and oriented ice crystals during the time of the measurement campaign. In order to estimate the quantitative fraction of randomly oriented hexagonal ice crystals, the HaloCam observations are combined with calibrated ground-based spectral radiance measurements to calculate the brightness contrast of the 22°-halo, i.e. the ratio of the measured radiance at the scattering angles 22° and 18° respectively. For these measurements SSARA (sun and sky automated radiometer)[1][2][3] was employed as a second instrument at CESAR and performed principle plane scans over a scattering angle range of 0°-50°. Since the radiance and brightness measurements also contain a contribution of the aerosol below the cloud, the sunphotometer measurements are used in addition to estimate the aerosol optical thickness.

Reason for choosing station

During the ACCEPT campaign multi-wavelength radar and lidar systems were operated with the objective to investigate particle size and shape in ice and mixed-phase clouds. The passive remote sensing observations using HaloCam and SSARA are complementary to these active remote sensing observations and provide an additional and independent estimate of ice particle shape and orientation in cirrus clouds. Thus, the collected dataset during the campaign offers a great opportunity to evaluate and compare the retrievals of ice particle shape and orientation from active and passive remote sensing.

Method and experimental set-up

Both instruments HaloCam and SSARA, operating during the ACCEPT/ICYHALO campaign, were tracking the sun and recording data every 2 and 10 seconds, respectively. With this set-up, a dataset of halo observations together with direct sun and scanning measurements was collected during the approximately 6 weeks of the campaign. This dataset provides statistical information about the frequency of halo displays during the campaign which indicate the occurrence of distinct ice crystal shapes and orientations in the observed cirrus clouds. The SSARA scanning mode was used to collect calibrated polarized[1)] measurements

1) In Oct 2012, SSARA was equipped with polarizing filters at 3 channels measuring at 500 nm.

of the radiance distribution of halo displays. This data may be used for a quantitative estimate of ice particle shape an orientation. Since the contrast of the 22°-halo for example is not only a function of the fraction of hexagonal ice crystals but also of the aerosol and cirrus optical thickness as well as the ice particle effective radius, further information is needed. The direct-sun measurements of the sunphotometer allow the retrieval of aerosol optical thickness during clearsky periods. Cirrus optical thickness and effective radius may also be derived from sunphotometer measurements in a second step using measurements in the near-infrared or in combination with radar and lidar measurements.

Preliminary results and conclusions

A first statistical evaluation of the halo displays observed during the ACCEPT/ICYHALO campaign are shown in Table 1. Out of about 14 days and 9 hours total observation time (during daylight only), cirrus clouds were observed in about 30% of the time and halos in about 10% of the total observation time. Relative to the time when cirrus clouds were observed, halos were present in about 27%.

The occurrence of the 3 different halos displays, that could be observed during the campaign, are displayed as a Venn-diagram, which reads as follows: observations of 22°-halos only are represented by the dark blue circle and sum up to an observation time of about 8 hours. Similarly, observations of sundogs (parhelia) are shown in light blue with a total time of about 11.5 hours. Upper tangent arcs are displayed in green and were observed for 3 minutes. These time periods represent observations of the respective halo display exclusively. Intersections between the 3 halo displays represent the time when two displays were observed simultaneously. For example 22°-halos together with sundogs occurred for about 2 hours of the total observation time. All three halo types were visible for about 6.75 hours.

Halo statistics	Observation time	Relative to total observation time
Total observation time	14 days 08:57:10 [hh:mm:ss]	100 %
Total cirrus observation time	04 days 14:08:00 [hh:mm:ss]	32 %
Total halo observation time	01 days 06:00:50 [hh:mm:ss]	9 %

Table 1: HaloCam statistics during ACCEPT/ICYHALO, from 09/10/-14/11/2014

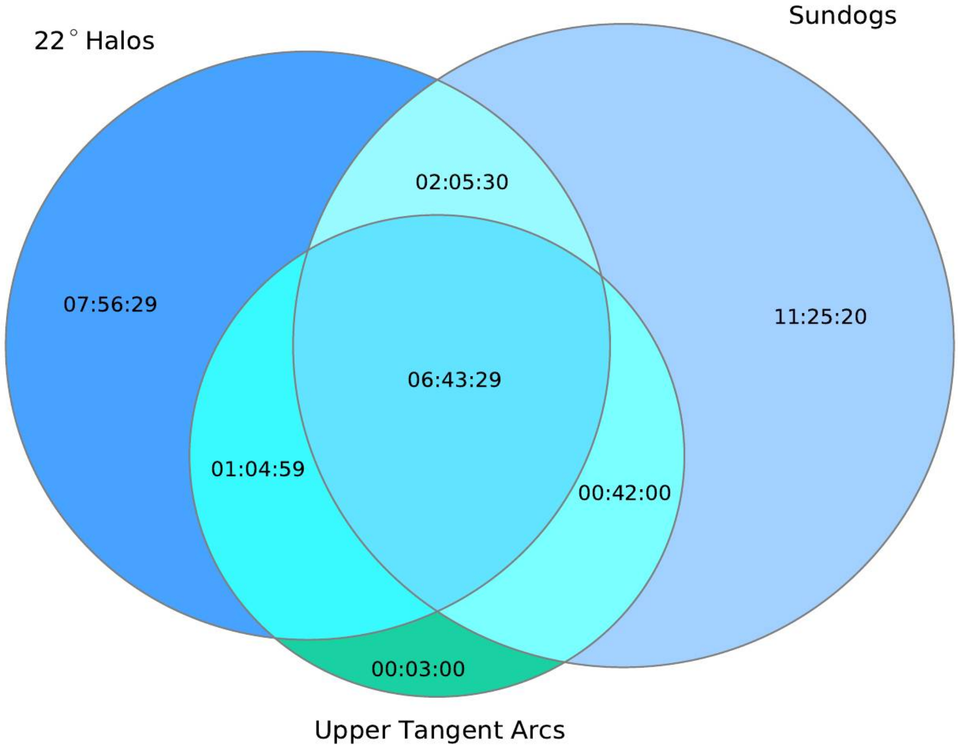

Figure 1: Halo display statistics during ACCEPT/ICYHALO, from 09/10/-14/11/2014

22°-halos are produced by refraction of sunlight by randomly oriented hexagonal ice particles.[4] Upper tangent arcs are formed by hexagonal columns which are oriented horizontally whereas sundogs are caused by horizontally oriented ice crystal plates.[4] The occurrence of each halo display can be linked with certain ice particle shapes and orientations. This information can be used for a further interpretation of the halo statistics during the campaign: about 30% of the observed ice clouds produced halos and thus contained some pristine hexagonal ice crystals. Further, halos that are produced by oriented particles (sundogs, upper tangent arcs) occurred for about 41% of the total time of halo observations, whereas only 27% of all halo observations indicate randomly oriented ice particles (22°-halo). Halo displays that were produced by a mixture of oriented and randomly oriented ice particles amount to about 36% of the total observation time. As a first conclusion, these observations indicate that the cirrus clouds that were observed during the 6 weeks-campaign contained about 30% of the time a certain amount of halo-producing ice crystals whereas the fraction of oriented particles exceeded the fraction of oriented particles.

During the campaign, continuous measurements were also performed with the SSARA sunphotometer. From these measurements, two different datasets were collected: direct-sun measurements with 12 spectral channels ranging from 340 nm to 1550 nm allow the retrieval of aerosol and cirrus optical thickness. The second dataset was obtained from almucantar (constant elevation) and principle plane (constant azimuth) scans, which will be used for further analysis to retrieve quantitative information about the fraction of ice particle shape and orientation.

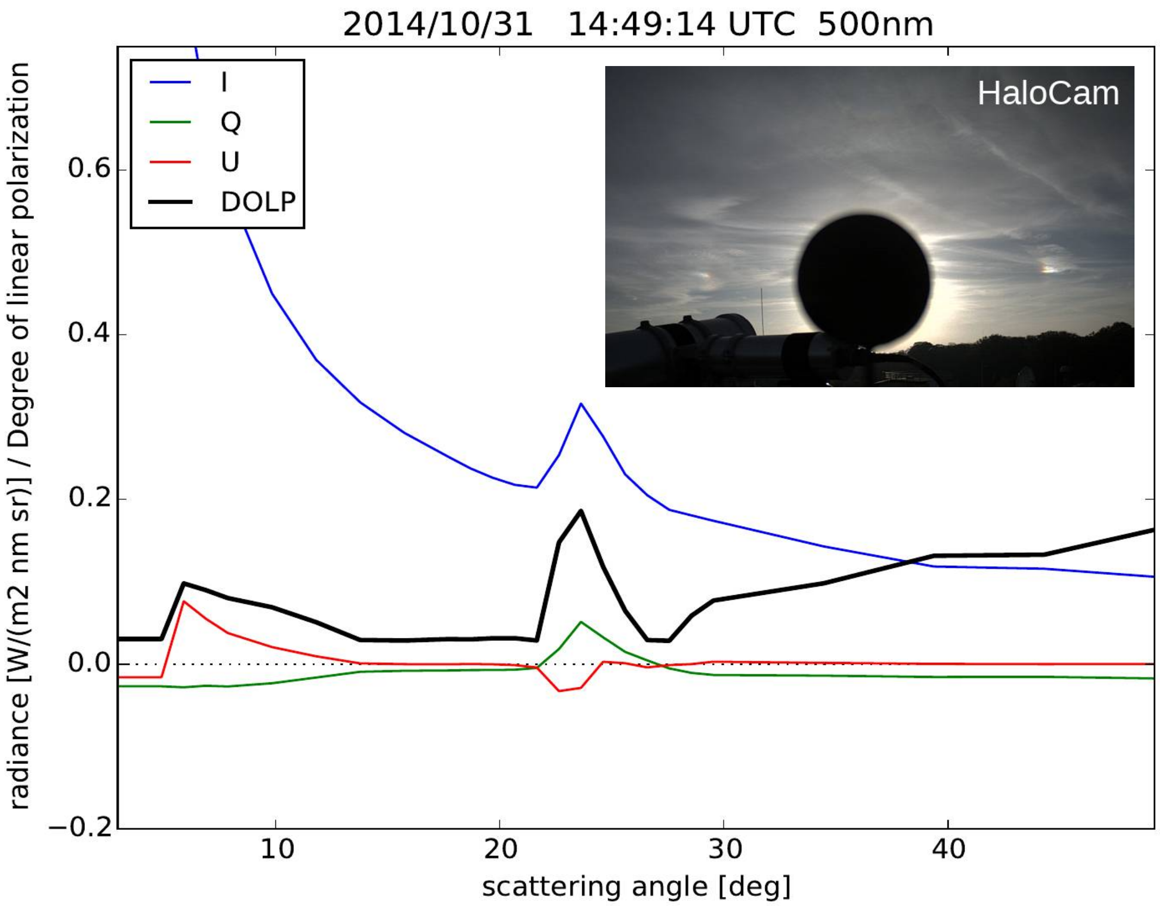

Abbildung 2: SSARA almucantar scan of sundog, 31/10/2014

From the scanning mode, measurements of three additional polarization channels (0°, 90°, 45°) at 500nm were evaluated. These 3 measurements allow to calculate the Stokes vector as well as the degree of linear polarization (DOLP).[5] Figure 2 shows preliminary data measured with the SSARA sunphotometer during the campaign in scanning mode. This data is only an example of a large dataset containing cross section scans of halo displays for several days during the campaign. The plot in Fig. 2 shows the radiance of the Stokes vector components I, Q, U [W/(m^2 nm sr)] and the degree of linear polarization (DOLP) [%] of an almucantar scan across a sundog as a function of scattering angle. The small picture inserted in Fig. 2 was recorded with HaloCam and shows this sundog at the instance of the scan. These quantitative measurements allow to retrieve quantitative information about the fraction of halo-producing ice particles, in this case oriented hexagonal plates cause the radiance peak at about 22° scattering angle.

Outcome and future studies

The continuous and high-quality dataset that could be collected thanks to the commitment of the 2 experts (Linda Forster and Markus Garhammer) engaged in the underlying TNA provides a valuable basis for qualitative and quantitative statistical analysis of halo displays and thus information about ice particle shape and orientation during the ACCEPT/ICYHALO campaign. Further detailed analysis of the ICYHALO dataset and comparison with the retrieved information about ice particle shape and orientation from the ACCEPT dataset will be realized by the ICYHALO project PI. It is planned to produce one publication about the data analysis of the ICYHALO project and one publication that compares the two independent methods using active (ACCEPT) and passive (ICYHALO) remote sensing to retrieve information about ice particle shape and orientation.

References

[1] Wagner, F., Schreier, M., Seefeldner, M., Rabus, D. and Koepke, P., 2003: SSARA – a new and accurate sunradiometer – suitable for measuring dust. Proceedings of the 2nd International Workshop on Mineral Dust, Paris, France.

[2] Toledano, C., M. Wiegner, M. Garhammer, M. Seefeldner, J. Gasteiger, D. Müller, and P. Koepke, 2009: Spectral aerosol optical depth characterization of desert dust during SAMUM 2006. Tellus B, 61 (1), 216–228, doi:10.1111/j.1600-0889.2008.00382.x.

[3] Toledano, C., et al., 2011: Optical properties of aerosol mixtures derived from sun-sky radiometry during SAMUM-2. Tellus B, 63 (4), 635–648, doi:10.1111/j.1600-0889. 2011.00573.x.

[4] http://www.atoptics.co.uk/halo/common.htm

[5] Hansen, J. E. and L. D. Travis, 1974: Light scattering in planetary atmospheres. Space Sci. Rev., 16, 527–610.